The Correlation of Active and Passive Microwave Outputs for the Skylab S-193 Sensor[1]

K. KRISHEN[2]

Abstract—This paper presents the results of the correlation analysis of the Skylab S-193 13.9 GHz Radiometer/Scatterometer data. Computer analysis of the S-193 data shows more than 50 percent of the radiometer and scatterometer data are uncorrelated. The correlation coefficients computed for the data gathered over various ground scenes indicates the desirability of using both active and passive sensors for the determination of various Earth phenomena.

I. Introduction

The recent years have seen steady growth of activity related to demonstrating the applicability of microwave sensors to the remote sensing of the Earth phenomena. Microwave sensors are especially attractive for the electromagnetic probing of the surface parameters, since they have the capabilities of penetrating foliage and the surface medium. Additionally, the data can be gathered independently of the natural light and in moderately adverse weather.

The relative advantages of using radiometers or radars are being investigated for many applications. In one of these studies, several examples have been given which point out that the interpretation of surface characteristics from microwave sensor outputs alone is more effective when data is available

1. Lockheed Electronics Company, Inc. Technical Report, LEC-7819, January 1976.

2. Formerly with Lockheed Electronics Company, Houston, Texas. Now with NASA/Johnson Space Center, Houston, Texas, 77058.

from both active (radar) and passive (radiometer) sensors [1]. The results of many experimental and theoretical studies showed the importance of using both active and passive sensors for remote sensing studies. Indeed this rationale was used in the specification of Skylab S-193 microwave system which consisted of both radiometer and active radar (scatterometer), in addition to, an altimeter. The operating frequency for S-193 was 13.9 GHz. A large volume of data has been acquired by NASA with the Skylab S-193 Radiometer/Scatterometer/Altimeter and L-band S-194 Radiometer Systems. Significant applications have already been shown with the Skylab microwave data [2, 3]. Future NASA programs have recognized the potential of using both active and passive microwave sensors and both will be used on the NASA SEASAT program.

In the interpretation of S-193 Radiometer and Scatterometer data taken over Great Salt Lake Desert site, a unique feature was noted[4]. The radiometer antenna temperature (T_A^o) and scatterometer backscattering cross section (σ_o) showed considerable dependence for a portion of the data, while some data showed a relative independence (Figure 1.). Further analysis of this data showed that for ground resolution cells where a considerable inhomogeneity existed (surface/subsurface water, and salt), the active and passive data were interdependent. This prompted the author to undertake a study of the correlation of S-193 Radiometer and Scatterometer data taken over several ground scenes during Earth Resources Experiment Package (EREP) passes.

Of the many data sets which were analyzed for possible correlations, more than 50 percent showed a high degree of independence of the scatterometer-measured σ_o and radiometer-measured T_A^o. This independence has not been verified theoretically since the formulation of the electromagnetic scattering from natural ground scenes poses many problems compelling the

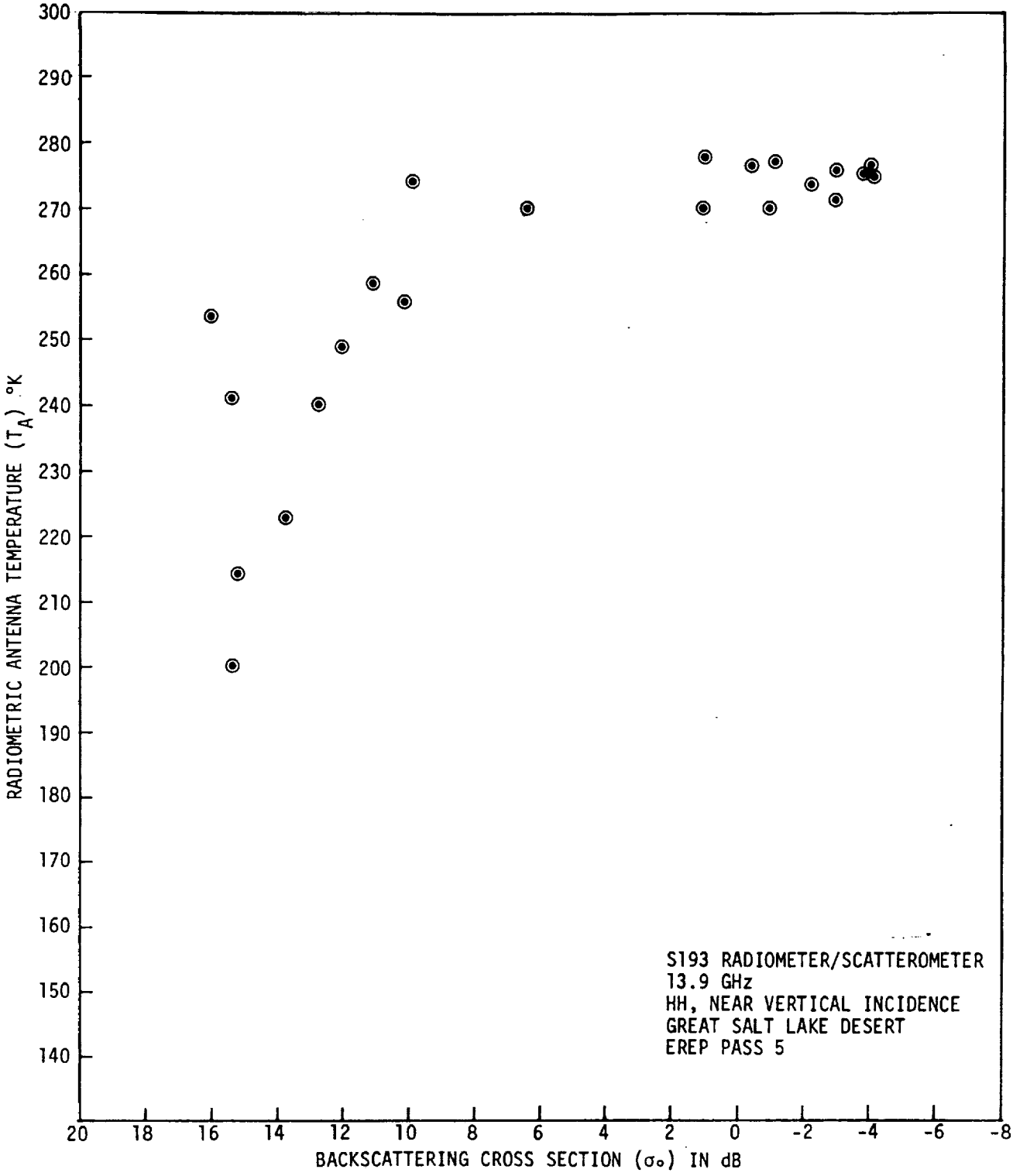

Figure 1. – The interdependence of S-193 radiometer and scatterometer data over Great Salt Lake Desert.

use of simplifications which render the final answers invalid. The results of the study presented in this paper suggest a clear advantage of using both active and passive sensors for the observation of Earth phenomena over scenes where several surface parameters are to be sensed (especially roughness, crop type, and soil moisture). However, if only the surface water bodies were to be identified, either a radiometer or a radar could be used with a side-looking synthetic aperture radar providing an advantage of higher resolution.

II. The S-193 Radiometer/Scatterometer Sensor Background

The radiometer and scatterometer operated at a frequency of 13.9 GHz in various scanning and polarization modes jointly and separately [5]. In the combined modes S-193 system measured nearly simultaneously the radiometric antenna temperature and radar backscattering cross sections over Earth's surface. The S-193 Radiometer/Scatterometer modes are given in Table I and briefly explained in this section. A detailed evaluation of the data is given in [6], [7], and [8].

Intrack Noncontiguous (ITNC) Mode

This mode is used for a joint radiometer and scatterometer operation. In this mode, only the pitch angle is varied. A resolution cell on the ground (Figure 2) is seen by the radiometer and scatterometer at approximately the following pitch angles: 0°, 15.6°, 29.4°, 40.1°, and 48°. The complete scan cycle time in this mode is 15.25 seconds. The roll angle is always zero. The selection of polarizations is given on Table I.

In reviewing the S-193 Radiometer/Scatterometer Skylab-acquired data, it was determined that some scan angle positions in this mode were different from the nominal prelaunch values. The angles, 0°, 15.6°, and 29.4°, are not markedly different. However, the 40.1° and 48° angles show noteworthy change. In particular, the last angle remains, for most part, within 46° to 47°. The 40.1° angle is within 1.5° of the nominal value.

TABLE I

Nominal Radiometer/Scatterometer Modes

Operation	Scanning mode choice	Polarization choice
Radiometer/scatterometer	1. Intrack Noncontiguous mode (ITNC)	1. Scatterometer VV, HH, VH, and HV* Radiometer V and H 2. One polarization combination (VV or HH or HV or VH) for scatterometer, and V or H for radiometer
Radiometer/scatterometer	1. Cross track Contiguous (CTNC) left/right 2. CTNC, left 3. CTNC, right	Same as for ITNC
Radiometer/scatterometer	1. Intrack Contiguous (ITC) mode	1. One polarization combination for scatterometer (VV or HH or VH or HV) and V or H for radiometer
Radiometer/scatterometer	1. Cross track contiguous (CTC)	1. VV or HH for scatterometer and V or H for radiometer
Radiometer only	1. CTC	1. V and H radiometer data
Scatterometer only	1. CTC	1. Scatterometer data for VV and HH

*Horizontal Transmit – Vertical Receive

On the Earth Resources Experimental Package (EREP) pass 40 the antenna gimbals malfunctioned. The ITNC mode was not used subsequently.

Crosstrack Noncontiguous (CTNC) Mode

In this mode, the roll angle is varied identical to the intrack noncontiguous mode on each side of the scan, and the pitch angle remains zero. The motion of the field of view (FOV) is shown in Figure 3, where it can be seen that individual cells are viewed from only one antenna position. Because of the motion of the antenna in the pitch direction, the cells lie on a curved arc. There are three forms of this mode – left scan, right scan, and left/right scan, as shown in the figure. The outermost cell is viewed at approximately 52° (corresponding to 48° gimbal angle) and the innermost cell at approximately 0° at all times. The total scan time for a complete cycle is 15.25 seconds. The selection of polarizations is identical to that of the ITNC mode (Table I).

The S-193 data for the CTNC mode shows that the antenna scan angles are approximately the same for 0°, 15.6°, and 29.4° angles. The 40.1° pitch angle reaches only approximately 37.5° for the Skylab-acquired data. The right scan extends up to approximately 43° instead of the nominal value of 48°, and the left scan extends up to approximately 46° instead of 48°. Some oscillation in the antenna pitch angle is also noticeable at each dwell angle. However, actual antenna angles were recorded. Skylab-4 mission antenna scan motion was also variable.

Intrack Contiguous (ITC) Mode

The pattern is similar to the intrack noncontiguous mode (Figure 4), except that the antenna is scanned much faster and there is no dwell at any antenna pitch angle. The entire inflight path is eventually scanned at all incidence angles corresponding to the five pitch angles of the ITNC mode, with this process.

The scan cycle time is chosen so that at the vehicle velocity the resolution cell at incidence angle 48° overlaps the previous cell by approximately 25 percent; the 40.1° cell overlaps its predecessor by less than 20 percent, etc., down to the 0° incidence angle case where gapping rather than overlap occurs. The complete cycle for one scan takes approximately 4.0 seconds.

As the vehicle progresses on successive scans, the entire path is viewed at 48° and less, except for gapping at lowest angles. Table I gives the selection of modes and polarizations.

In the ITC mode, the starting angle was about 43° (the nominal prelaunch value was 48°) during the Skylab-2 and -3 missions. Since the Doppler filters are centered around 48°, the scatterometer data recorded for 43° is highly attenuated. Corrections for the Doppler filter attenuation have been implemented into the S-193 processing program. Other angles are also slightly off. The difference increases with increasing pitch angle. However, no correction to the scatterometer data is needed at the angles other than the highest angle (approximately 43°).

During the Skylab-3 mission, a malfunction occurred in the antenna gimbals. The pitch gimbal was disabled as a fix. Consequently, no data was gathered in the ITC mode after the fix.

Crosstrack Contiguous (CTC) Mode

This mode contains three submodes and further selection of polarizations (see Table I). It provides a side-to-side linear scan covering ±11.375° and a turnaround to repeat. As can be seen in Figure 5, this is a mapping mode. To compensate for the satellite forward velocity which could cause skewing of the pattern perpendicular to the flightpath, the pitch gimbal is scanned backwards slightly as the roll angle oscillates between

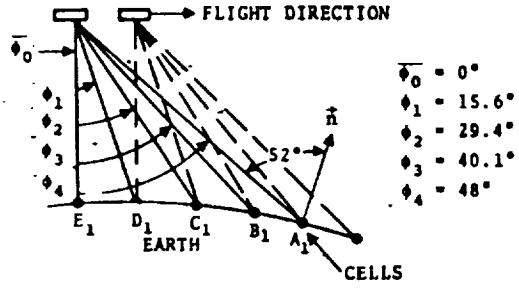

Figure 2. – Intrack noncontiguous (ITNC) scan mode ($\hat{n}$ is the normal to the surface at point A_1).

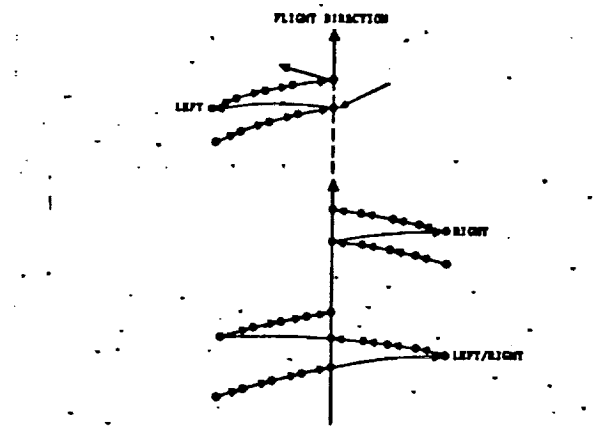

Figure 3. – Crosstrack noncontiguous (CTNC) mode.

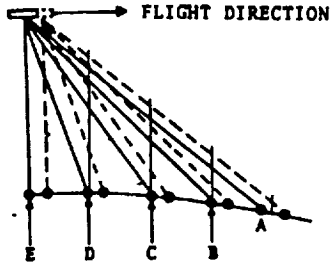

Figure 4. – Intrack contiguous (ITC) mode.

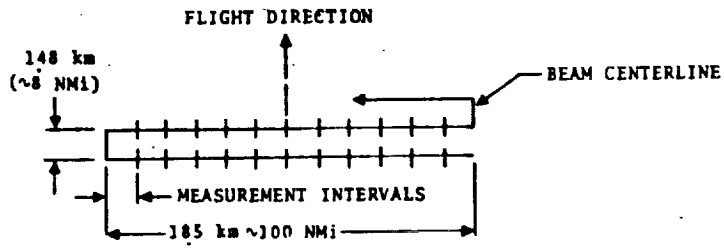

Figure 5. – Crosstrack contiguous (CTC) mode.

its limits. Measurements are made for every 1.896° of beam center motion, ranging from -11.375° to +11.375° in roll. The total time of one cycle is 4.24 seconds. The pitch offset angles for this mode can be chosen as 0°, 15.6°, 29.4°, or 40.1°. The roll offset angles can be chosen from 0°, +15°, -15°, -29.4°, and +29.4°. Either pitch or roll offset angle is selectable.

A study of Skylab-acquired data in the CTC mode revealed that the scan extends only up to a total of approximately 20.6° instead of 22.75°. The repeatability of the timing sequence also differs from that indicated by Figure 5.

Because of the antenna malfunction during the Skylab-3 mission, the pitch gimbal was pinned at 0°. Consequently, the ground scans are not parallel for the Skylab-4 (SL-4) mission. The roll angles are also different in SL-4 data.

III. Data Analysis Discussion

The correlation study was conducted on data gathered with various radiometer/scatterometer modes. Data corresponding to a particular ground cell was sorted for each polarization. The correlations were computed on a set of pairs of radiometer/scatterometer values. Each pair corresponds to a specific ground cell and incidence angle (θ). Values of radiometric antenna temperature (T_A^o) for which radar backscatter (σ_o) values did not exist were not used. For instance, in the ITC mode, the pair of data was the σ_o and the T_A^o following immediately after the σ_o for a particular θ.

For each set of data corresponding to a test site a least-square polynomial fit is used to determine the coefficients of the equation

$$\text{Rad} = \sum_i a_i \, (\text{Scat})^i \qquad (1)$$

where Rad is the radiometric antenna temperature, and scat is the value of σ_o (not in dB). The magnitude of correlation coefficient is then computed by using

$$R = \left[\left(\sum_{1}^{N} (Ral - \overline{Rad})^2\right) \Big/ \sum_{1}^{N} (Rad - \overline{Rad})^2\right]^{1/2} \qquad (2)$$

where

Ral = the value of T_A for each σ_o calculated from least-squares polynomial (1)

Rad = the value of T_A corresponding to σ_o used to calculate Ral

$\overline{Rad}$ = the average value of T_A

N = the number of pairs of σ_o, T_B values used in the correlation study.

The ground scenes over which the correlation study was conducted consisted of homogeneous land and water surfaces, as well as, those which contained surface inhomogeneities. Deep space was considered an excellent "no backscatter" target. The analysis of σ_o and T_A^o allowed to study the instrument caused correlations in the data stream. Test sites homogenoeus in both dielectric properties and surface roughness were selected to study interdependence of σ_o and T_A^o for such targets. The homogeneity of these targets was ascertained by reviewing ground data measurements, in addition to, the Skylab and aircraft acquired data[6]. Additionally, data for test sites with biomass cover, bare ground, and water was also analyzed. The data used in the correlation study encompasses a wide range of σ_o and T_A^o values.

IV. Results of the Correlation Analysis

The results of the computer analysis of the radiometer/scatterometer data are given in Table II. This table also contains pertinent site description, S-193 mode, and range of

TABLE II

Correlation Coefficients For S193 Radiometer/Scatterometer Data

EREP pass/day of year	GMT time from/to	Site/description	S-193 mode and polarizations	Range of angle of incidence	Average T_A^o	Correlation coefficient R
LC2/224	15:47:11.67 to 15:49:10.69	Deep space	CTC R/S, HH scat H rad	N/A	14.97	0.28
LC1/165	15:42:11.54 to 15:44:10.72	Deep space	CTC R/S, HH scat H rad	N/A	13.15	0.09
5/156	17:57:33 to 17:58:33	Great Salt Lake Desert, Utah (smooth surface, large dielectric changes)	CTC R/S, HH scat H rad	1° to 12°	257.64	0.48
15/217	16:37:39 to 16:38:20	Kansas	CTC R/S, HH scat H rad	32.7° to 34.1°	279.12	0.31
21/244	15:36:5.5 to 15:36:51.08	Mali/Algeria	CTC R/S, VV scat V rad	1° to 12°	284.824	0.18
5/156	18:02:34 to 18:07:10	Gulf of Mexico	ITNC/ VV scat V rad (showers for very small portion of field of view)	1° to 51.3°	162.12	0.45
5/156	18:02:34 to 18:07:10	Gulf of Mexico	ITNC/ HH scat H rad	1° to 51.3°	139.08	0.31
8/162	15:20:20.85 to 15:23:50	Gulf of Mexico	ITNC/ VV scat V rad (rain for very small part of field of view)	1° to 51.3°	152.63	0.56
8/162	15:20:20.85 to 15:23:50	Gulf of Mexico	ITNC/ HH scat H rad (rain for very small part of field of view)	1° to 51.3°	125.95	0.43
22/245	14:57:27.11 to 14:59:40.88	Mediterranean Sea/Malta/Italy land/water	CTC R/S, VV scat V rad	1° to 12°	135.25	0.69
22/245	14:52:40.89 to 14:57:27.05	Algeria/Tunisia	CTC R/S, VV scat V rad	1° to 12°	285.18	0.04
22/245	14:48:21.3 to 14:52:40.56	Sierra Leone/ Guinea/Mali	CTC R/S, HH scat H rad	1° to 12°	278.98	0.17
14/217	14:55:13.8 to 15:01:54	British Columbia Montana/North Dakota/Minnesota/ Wisconsin (very little water)	ITNC VV scat V rad	1° to 51.3°	261.5	0.45
			HH scat H rad		254.7	0.16
LC3/254	13:53:6.16 to 13:55:0.68	Deep space	CTC R/S, HH scat H rad	N/A	14.5	0.14
6/160	15:07:32 to 15:08:12.3	Nebraska/Missouri	CTC R/S, HH scat H rad	20° to 42°	289.01	0.23

TABLE II (Concluded)

Correlation Coefficients For S193 Radiometer/Scatterometer Data

EREP pass/day of year	GMT time from/to	Site/description	S-193 mode and polarizations	Range of angles of incidence	Average T_A^o	Correlation coefficient R
15/217	16:57:44.86 to 17:00:0.5	Brazil/South Atlantic land/water	CTC R/S, HH scat H rad	32.7° to 34.1°	177.3	0.99
10/164	14:11:46 to 14:13:55	Brazil/South Atlantic land/water	CTC R/S, VV scat V rad	32.7° to 34.1°	183.5	0.99
13/216	17:19:50.8 to 17:20:46.2	Colorado/Kansas	CTC R/S, VV scat V rad	17° to 21°	272.13	0.87
11/165	14:42:6.4 to 14:43:45.6	Nevada/Utah/ Arizona	CTC R/S, VV scat V rad	32.7° to 34.1°	279.61	0.71
12/215	17:59:11.54 to 18:00:40.43	Oregon coast land/water	CTC R/S, HH scat H rad	1° to 12°	268.63	0.76
13/216	17:25:18.1 to 17:27:0.77	Gulf of Mexico and Cuba land/water	CTC R/S, VV scat V rad	1° to 12°	143.3	0.67
5/156	18:00:12.7 to 18:01:15.7	New Mexico/Texas (rained earlier)	CTC R/S, HH scat H rad	32.7° to 34.1°	277.1°	0.65
8/162	15:20:20.8 to 15:24:7.5	Gulf of Mexico/ British Honduras (land/water)	ITNC R/S, VV scat V rad	1° to 51.3°	151.25	0.59
			HH scat H rad		123.54	0.27
13/216	17:25:36.8 to 17:26:21.3	Gulf of Mexico	CTC R/S, VV scat V rad	1° to 12°	130.6	0.33
29/252	19:25:6.7 to 19:33:51.4	North Atlantic	ITNC VV scat V rad	1° to 51.3°	143.9	0.34
			HH scat H rad		119.8	0.25
21/244	15:14:36 to 15:20:1	Argentina/Uruguay South Atlantic (land/water)	CTC R/S, VV scat V rad	1° to 12°	199.1	0.76
22/245	14:52:40.9 to 14:59:41.00	Algeria/Tunisia/ Mediterranean Sea land/water	CTC R/S, VV scat V rad	1° to 12°	151.72	0.80
16/224	16:07:39 to 16:09:07	Gulf of Mexico	CTNC left HH scat H rad	0.2° to 49°	125.9	0.4
16/220	16:4:54 to 16:7:02	Gulf of Mexico	ITNC VV scat V rad	.85° to 50°	204.72	0.4
11/165	14:47:33 to 14:48:29	Gulf of Mexico	ITC VV scat V rad	1° to 52°	207	0.49

angles of incidence. Average radiometric antenna temperature is also included to provide an indication of the average reflectivity of the test site, since the approximate value of reflectivity R(0) can be computed from the equation:

$$T_A = L_2\left[T_s|R(o)|^2 + (1 - |R(o)|^2)T_g\right] + T_{ATM} \qquad (3)$$

where L_2 is the transmittance of the atmosphere, T_A is the radiometric antenna temperature, T_s the sky background temperature, T_g the ground temperature, and T_{ATM} the radiometric temperature of the atmosphere.

Before the interpretation of the values of R (the correlation coefficient) is presented, the following remarks about the three classes of targets examined for correlation will be made as follows.

Deep Space

The values of R for deep space range from 0.09 to 0.28. Although only three data segments are listed in Table II many others were examined and R values were found to be within this range. The independence of radiometer and scatterometer data is expected for deep space since the scatterometer data, in this case, is the system noise measured after a finite time from the noise measurement given in the radiometer data. The active and passive outputs represent two independent samples of noise. This result is encouraging, since it points to very low leakages between radiometer and scatterometer systems. Thus the high correlations in Table II are scene-caused rather than instrument-caused.

Homogeneous Land/Water Sites

The test sites for which the reflectivity values exhibit a small standard deviation are considered uniform in dielectric properties. The details of the selection of these sites are given in [6] where ground data and support flight data was examined to ascertain the uniformity of the test site.

For example, the homogeneity of the dielectric properties for EREP pass 5 can be assessed by analyzing the L-band S-194 Radiometer data. For this vertical-looking sensor, the effects of ocean surface wind velocity (which varies from 9 to approximately 16 knots within one sigma standard deviation) is negligible. The measured antenna temperature varies from 105.9 to 105.0°K over a period from GMT 18:03:32.35 to 18:04:36.56. These radiometric temperatures have a constant offset because of sun angle correction. This correction will reduce all temperatures by a few degrees. The standard deviation for 184 data samples is less than 0.3°K.

Of the several land data segments analyzed only a few showed uniformity of the dielectric properties. The data for EREP passes 6, 14, and 22 are given in Figures 6, 7, and 8, respectively. The S-193 Radiometer, as well as, S-194 Radiometer data show small deviation in the values of antenna temperatures. On the other hand, the Great Salt Lake area (EREP passes 5 and 11) shows a large variation in the surface parameters (specifically the dielectric properties). Figures 9 and 10 show this variation. Similar observations followed for other land sites of Table II which show a higher correlation coefficient R. The high value of R for the EREP pass 13 (GMT 17:19:50.8 to 17:20:46.2) is indicative of the high sensitivity of the radiometer, as well as, the scatterometer to the soil moisture variations in the angular range, 17° to 21°.

Inhomogeneous Land/Water Site

Several data segments taken over sites with differing biomass cover typified by the presence of large bodies of water were examined for correlation study. The presence of water with the field of view over extended test sites gives a wide range of values of σ_o and T_A^o (Figure 11). In all cases involving inhomogeneous ground scenes the correlation coefficients, R, turned out to be high. The presence of rain or rain soaked soil constituted

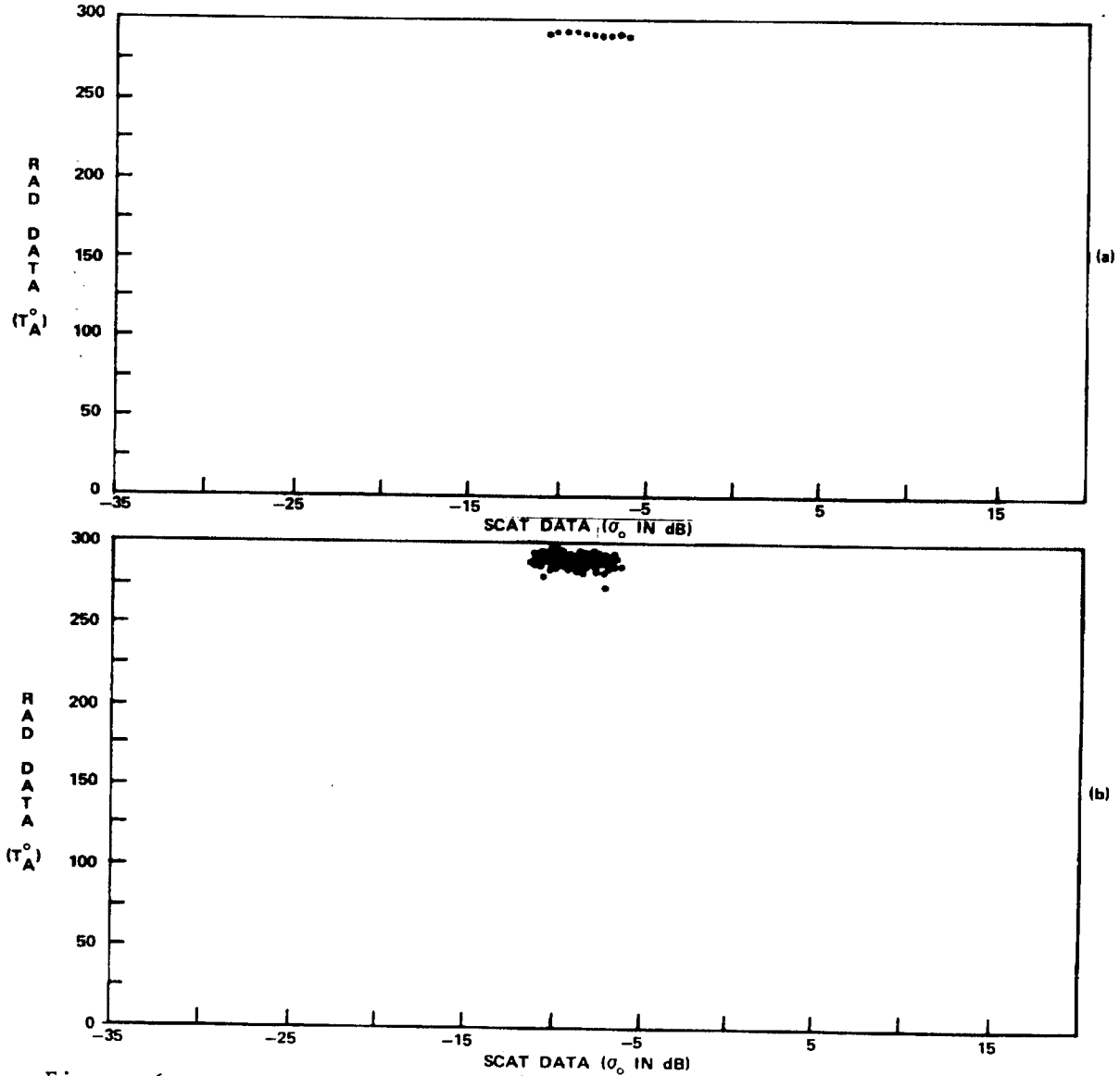

Figure 6. – S-193 Rad/Scat data for EREP pass 6, GMT 15:07:32·068 to 15:08:12·286, CTC (a), plot of Ral (b), actual data.

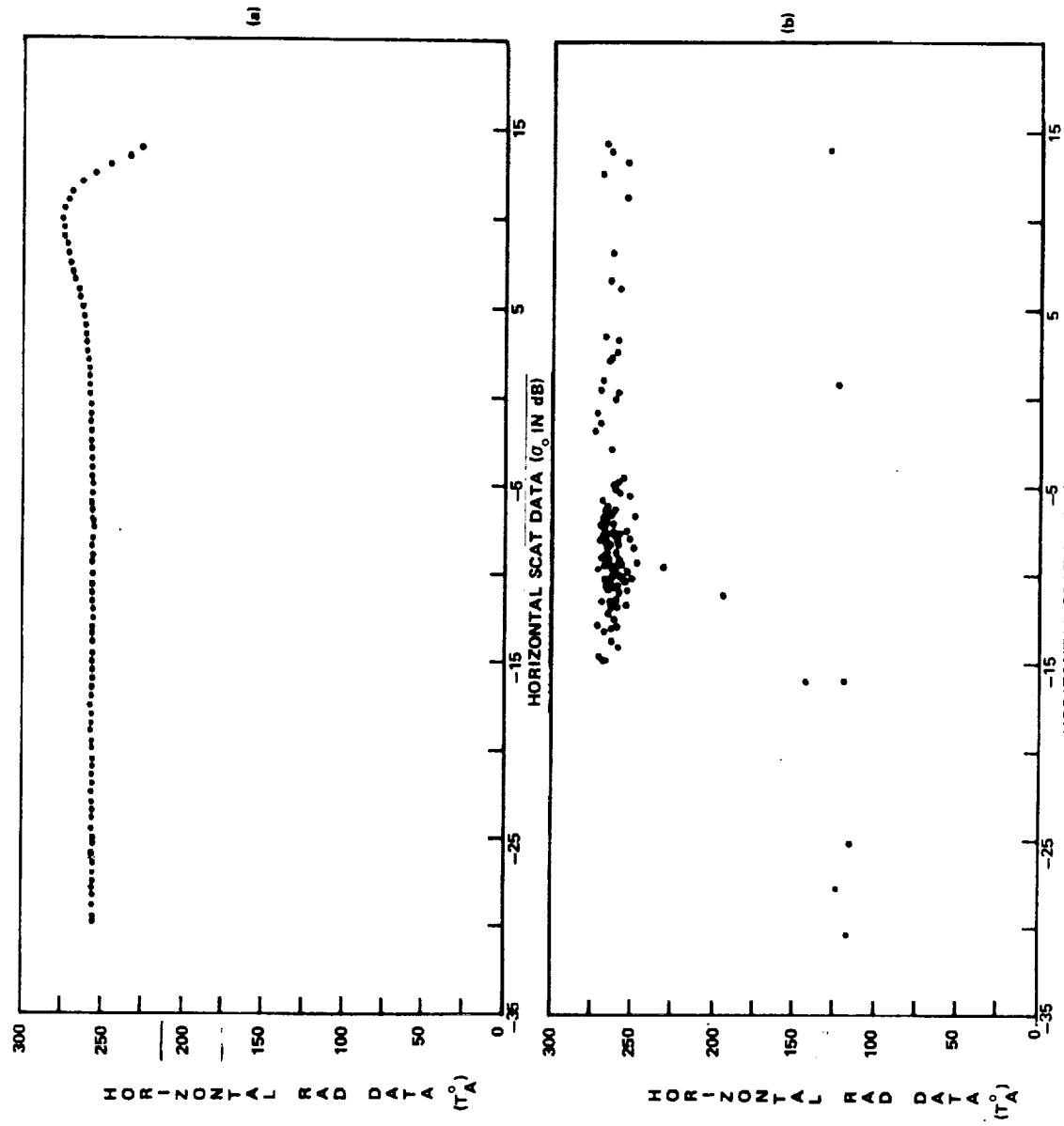

Figure 7. – S-193 Rad/Scat data for EREP pass 14, GMT 14:55:13·8 to 15:01:53·96 ITNC (a), plot of Ral (b), actual data.

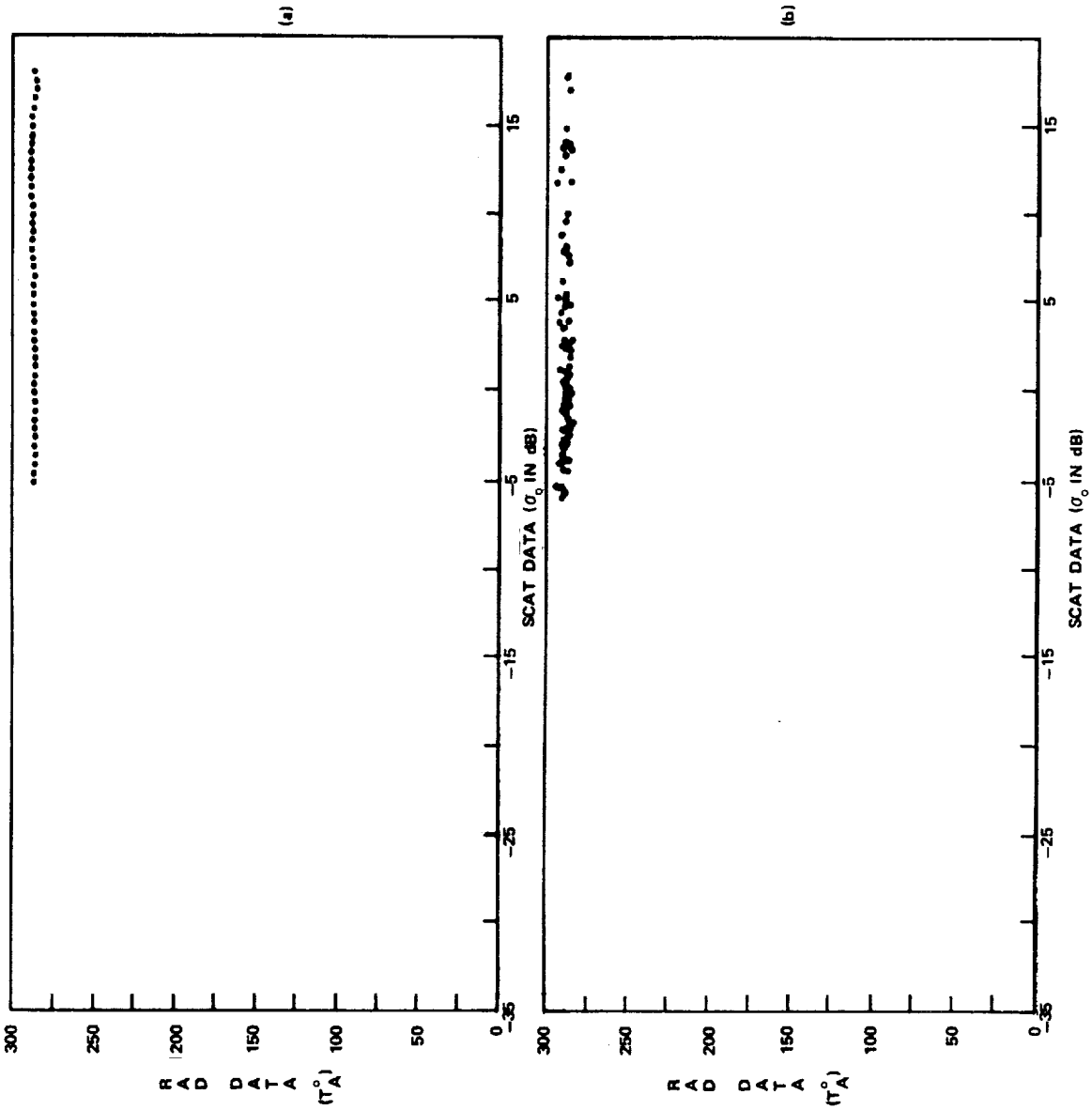

Figure 8. — S-193 Rad/Scat data for EREP pass 22, GMT 14:52:40.9 to 14:57:27.05, CTC (a), plot of Ral (b), actual data.

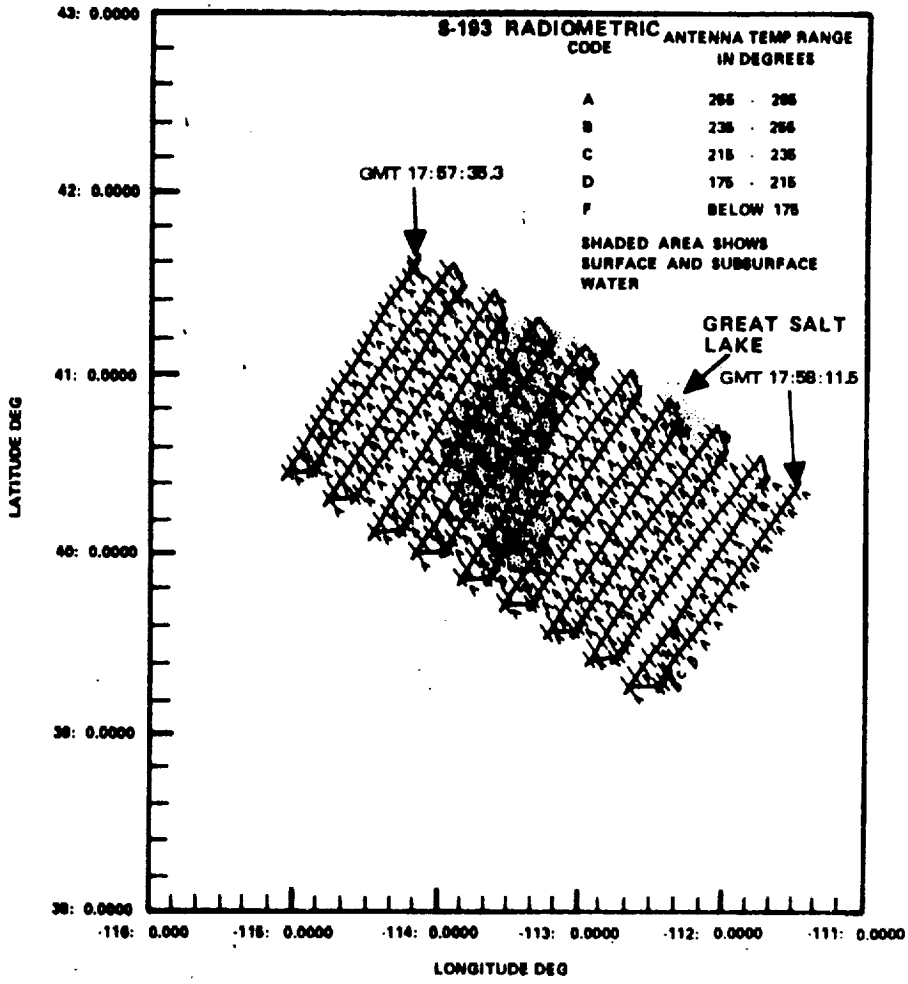

Figure 9. — Field of view and S-193 Radiometer antenna temperature distribution over GSLD (pass 5).

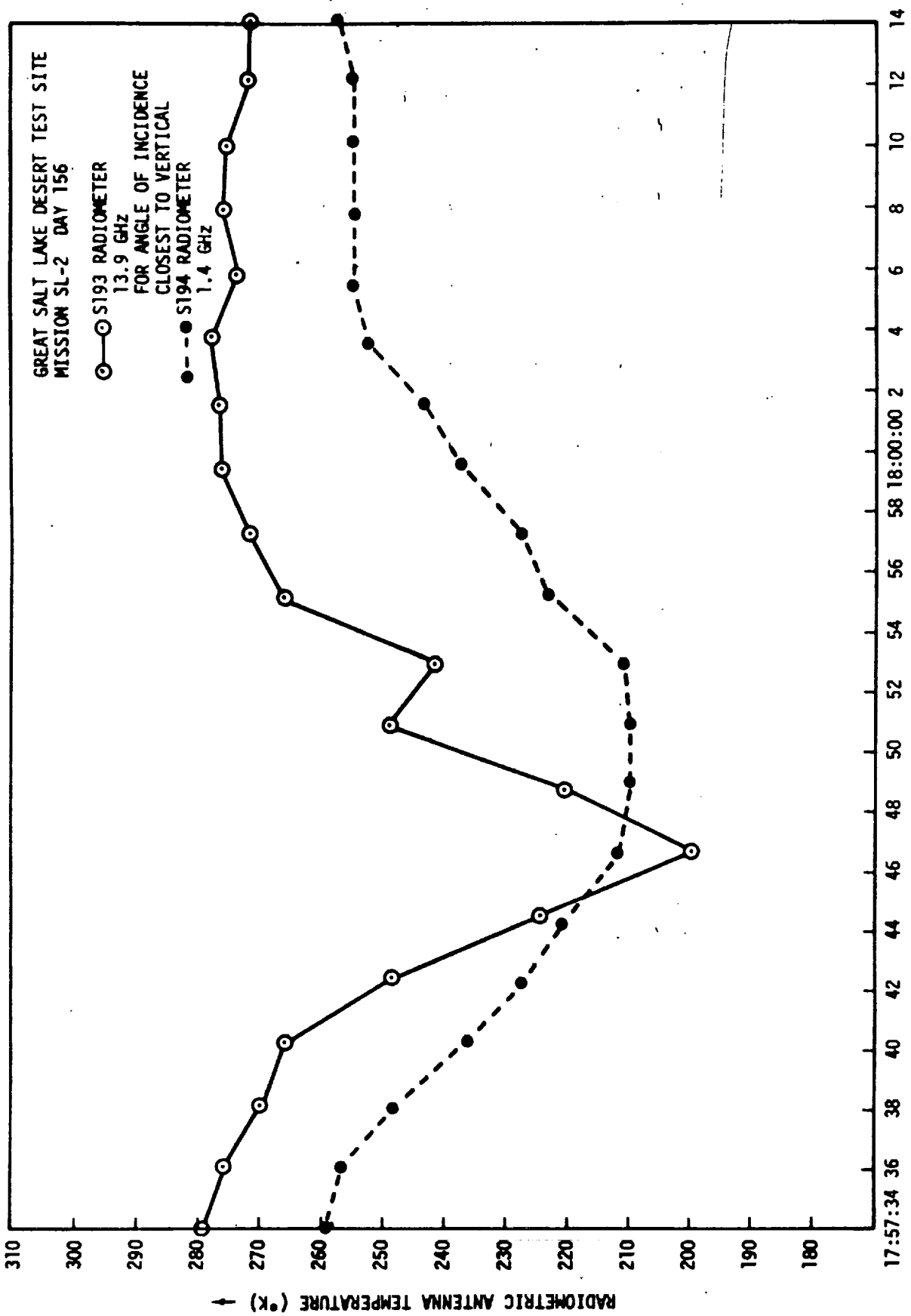

Figure 10. — Comparison of S-194 and S-193 Radiometric antenna temperatures (nearly vertical incidence) for GSLD.

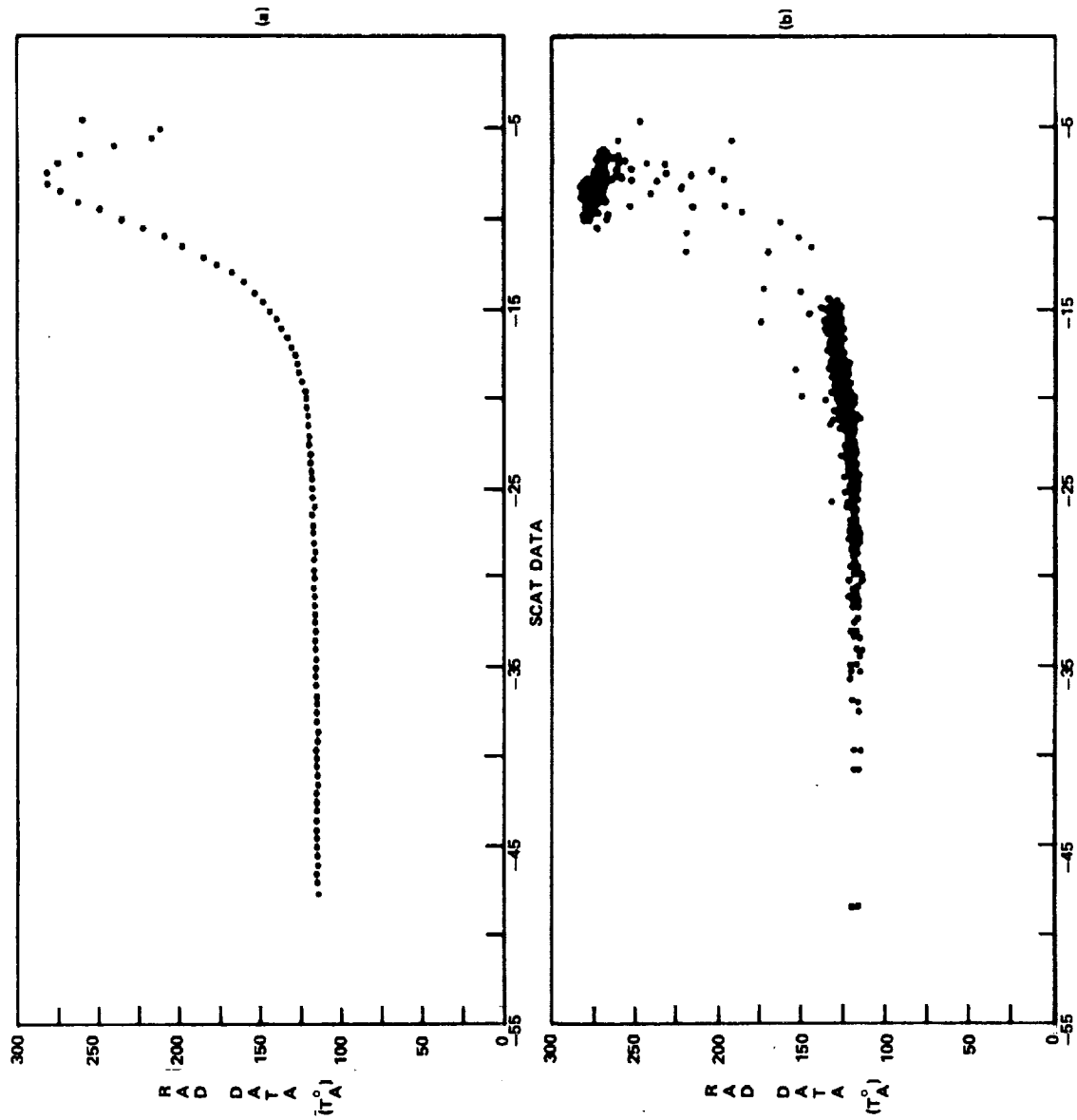

Figure 11. — S-193 Rad/Scat data for EREP pass 15, GMT 16:57:49·86 to 17:00:0·5004, CTC (a), plot of Ral (b), actual data.

an inhomogeneous target (example, pass 5, GMT 18:00:12.7 to 18:01:15.7).

V. Data Interpretation and Conclusions

To facilitate data interpretation, Figures 12 and 13 were drawn from the data presented in Table II. For the CTC mode high values of R belong invariably to ground scenes which have surfaces consisting of a wide range of dielectric properties. Thus the gross surface inhomogeneities can be observed by active and passive systems equally well. A similar conclusion follows for the other modes. Thus for a particular angle of incidence, the response to large changes in surface dielectric properties is similar for active and passive systems. Low values of R are observed for sites which do not contain both land and water or have a wide variation in surface properties. The independence of active and passive data for these sites indicate a strong dependence of active microwave sensor to the surface roughness and slope distribution.

Over the water sites the scatterometer provides a more sensitive system to measure surface roughness compared to the radiometer [2]. For high sea states, however, the radiometer shows higher sensitivity due to the formation of foam [2]. The results of the correlation study point to the need of having both active and passive systems to observe various surface parameters over land or ocean scenes. The desirability of conducting space experiments with both active and passive systems is amply demonstrated by the data presented in Table II. Of the 33 values of R, 21 are less than 0.5, suggesting independence of the radiometer and scatterometer data at 13.9 GHz. Indeed for NASA/Johnson Space Center soil moisture studies this has been recognized and both active and passive sensors are being employed.

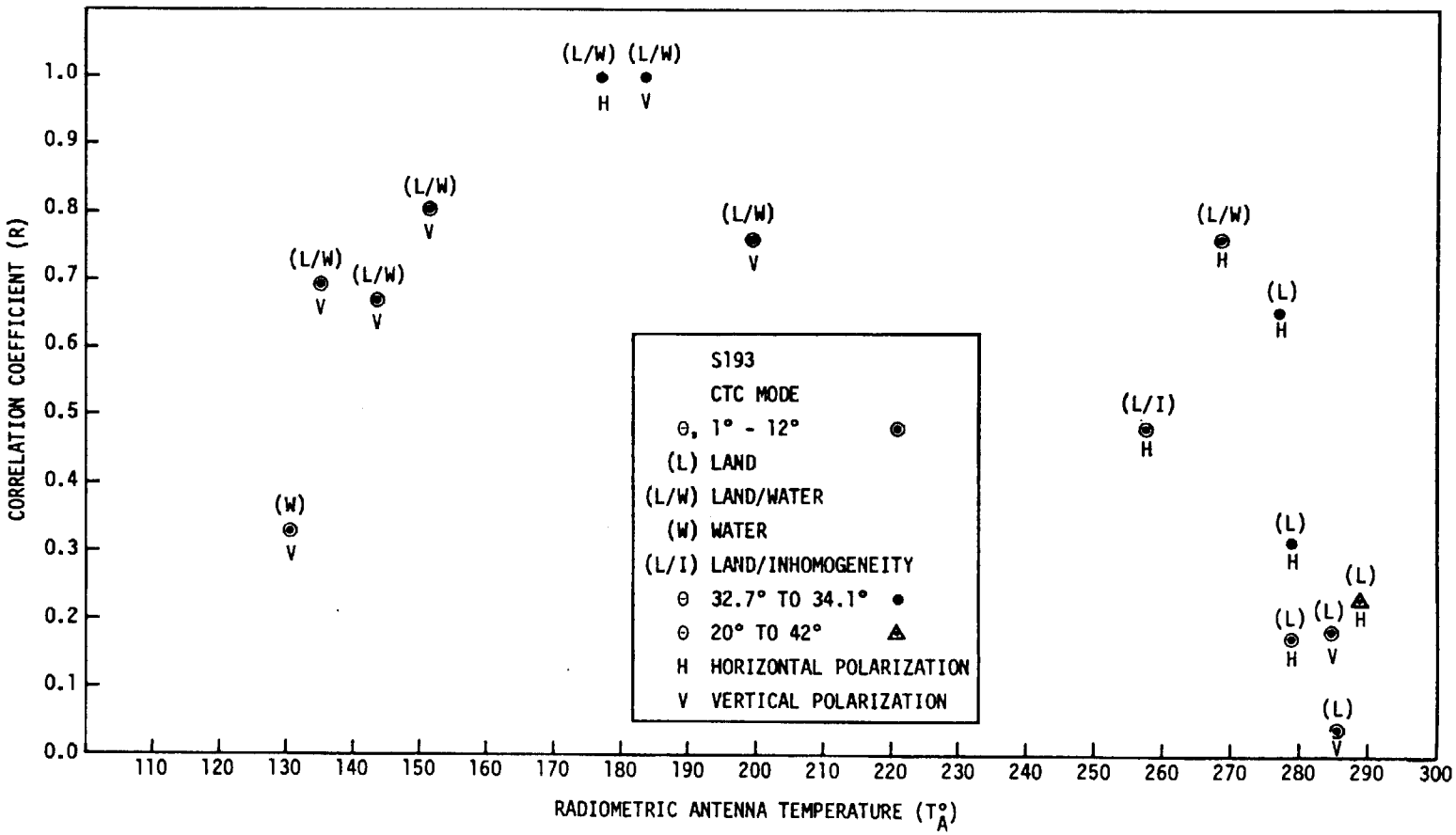

Figure 12. — Values of correlation coefficient R for CTC mode.

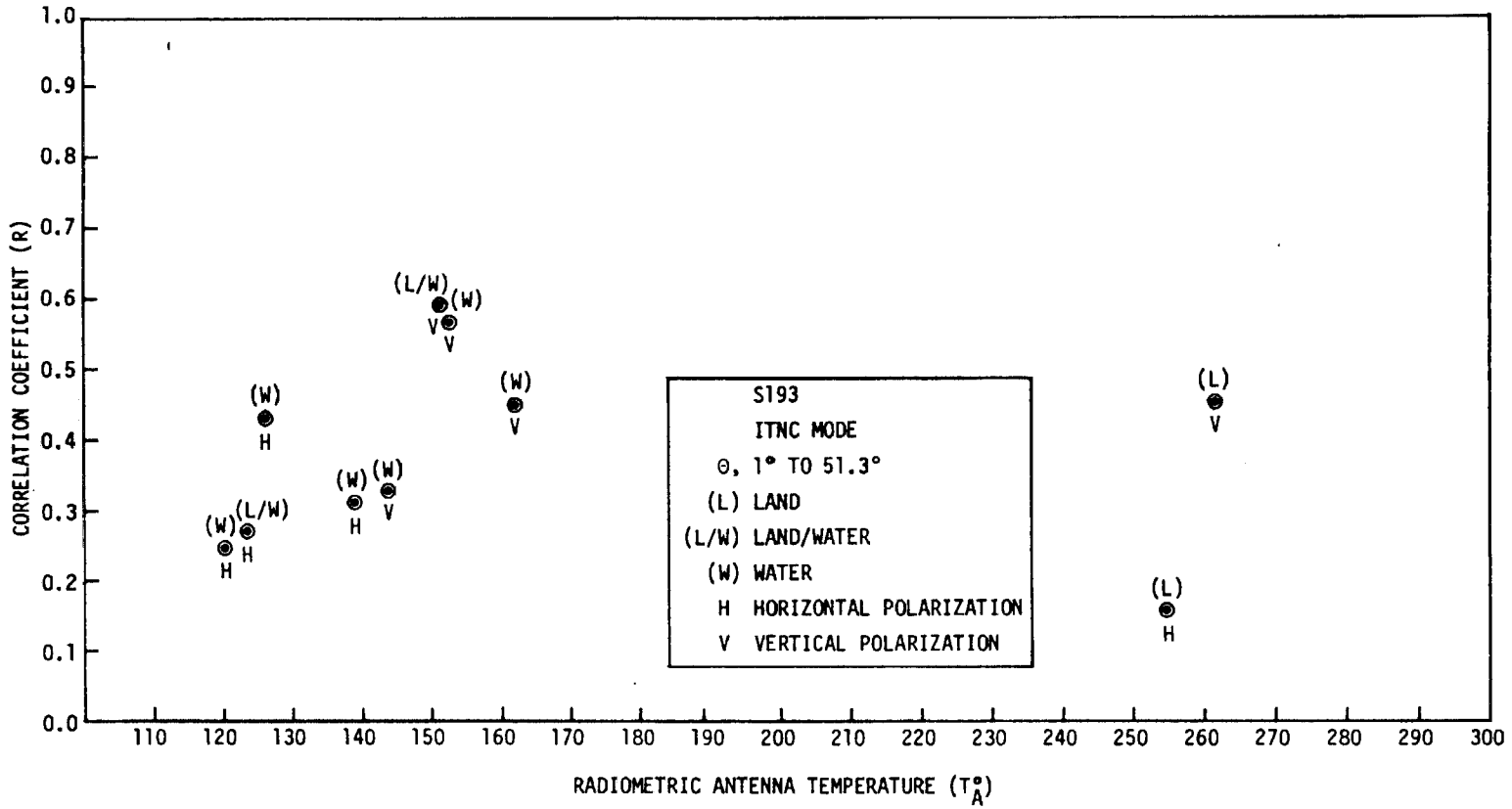

Figure 13. – Values of correlation coefficient R for ITNC mode.

References

[1] Peake, W. H.; Shultz, C. H.; and Riegler, R. L.: "The Mutual Interpretation of Active and Passive Microwave Sensor Outputs." Technical Report 1903-3, Ohio State University, July 1966.

[2] Active Microwave Workshop Report. National Aeronautics and Space Administration, NASA SP-376, Washington, D.C., 1975.

[3] Krishen, K.: "The Significance of the S-193 Skylab Experiment Using Preliminary Data Evaluation." Lockheed Electronics Company, Inc., Technical Memorandum LEC-4250, August 1974.

[4] Krishen, K.: "Remote Sensing of Surface Parameters Using Skylab S-193 Radiometer/Scatterometer Data." Proceedings of the URSI Specialist Meeting on Microwave Scattering and Emission from the Earth, University of Berne, Berne, Switzerland, September 1974.

[5] Historical Logbook, S-193 Microwave Radiometer/Scatterometer/ Altimeter. General Electric Corporation, Document Number 72SD4234, Revision A, Volumes 1 through 10, October 1972.

[6] Krishen, K.; and Pounds, D. J.: "S193 Scatterometer Backscattering Cross Section Precision/Accuracy For Skylab-2 and -3 Missions (Sensor Performance Evaluation Task SPE-S193-004)." LEC-6119, Lockheed Electronics Company, Inc., Houston, Texas, June 1974.

[7] Pounds, D. J.; and Krishen, K.: "S193 Radiometer Brightness Temperature Precision/Accuracy For SL-2 and SL-3 (SPE-S193-012, S~AD)." LEC-5976, Lockheed Electronics Company, Inc., Houston, Texas, June 1975.

[8] NASA/Johnson Space Center, Earth Resources Experiment Package Sensor Performance Evaluation Final Report. Volume IV (S-193 Radiometer/Scatterometer), MSC-05546, January 1975.